Title: Initiation of acute Graft-versus-Host Disease by Angiogenesis

Supplemental Data

Supplemental Material and Methods

Protein quantification by dimethylation labeling

Cells were digested in solution and labeled by dimethylation according to Boersema *et al.*[21] Endothelial cells were pelleted and were resuspended in 75 µl of denaturation buffer [6M urea (Sigma-Aldrich), 2M thiourea (Sigma-Aldrich), 10mM HEPES (pH=8)]. They were sonicated 30 pulses of limit microtip sonication at 30% on duty cycle. The remained cell pellet was erased by centrifugation at 14000 rpm for 15 minutes. After removing the supernatant, the protein concentration was calculated by Bradford. Each sample had 15-20 µg of protein (approximately 0.4 mg/ml). They were reduced by incubating with 5 µl of 10mM *tris*(2-carboxyethyl)phosphine (TCEP) (Sigma-Aldrich) for 30 min at RT, followed by an alkylation step using 5 µl of 55mM Cloroacetamide (Sigma-Aldrich) for 60 min at RT. The samples were first digested using 0.25 mg/ml endopeptidase LysC (Wako, Osaka, Japan) for 3 hours. The samples were diluted by adding 100 µl of 50 mM ammonium bicarbonate (pH=8.5), and finally digested with 0.25 mg/ml trypsin (Promega, Germany) for 16h. The digestion was stopped by acidifying each sample to pH<2.5 by adding 10% trifluoroacetic acid solution. The peptide extracts were purified and stored on stage tips according to Rappsilber *et al.*[22] The samples were reconstituted in 100 µl of 20 mM HEPES buffer pH=7.5. The samples were differentially labelled adding 8 µl of 8% of light label formaldehyde (Pierce, Thermo Scientific) in ECV (+28Da), medium label formaldehyde (Cambridge Isotope Laboratories) (+32Da) and heavy label formaldehyde (Sigma-Aldrich, Germany) (+36Da) cells (45). We added 8 µl of 0.6M $NaBH_3CN$ (Sigma-Aldrich, Germany) to the light and medium labelled samples and 8 µl of 0.6M $NaBD_3CN$ (Sigma-Aldrich, Germany) to the heavy labelled simple, incubating at 20ºC. The reaction was quenched after 1 hour adding 30 µl of 1% ammonia solution. All the samples were mixed and acidified to pH<2.5 by adding 10% trifluoroacetic acid solution.

High through-put LC-MS/MS analysis

After Stage-Tip extraction, the eluted peptides were lyophilized and resuspended in 1% trifluoro-acetic acid and 3% acetonitrile buffer. Peptides were separated on a Eksigent nLC-415 system (Eksigent Technologies, CA), resolved with a reversed-phase column (30 cm in length, 75 mm ID [inner diameter of the fused silica capillary tubing used to make the column], 3 mm, Dr.

Maisch GmbH C18) by a gradient from 4 to 42% B in 240 min. MS and MS/MS spectra were analysed coupled to a QExactive mass spectrometer (Thermo Scientific). The mass spectrometer was operated in a data-dependent acquisition mode with dynamic exclusion enabled (30 s). Survey scans (mass range 300-1700 Th) were acquired at a resolution of 70,000 with the ten most abundant multiply charged (z ≥ 2) ions selected with a 4 Th isolation window for HCD fragmentation. MS/MS scans were acquired at a resolution of 17,500 and injection time of 60 ms.

Processing of mass spectrometry data

Protein and peptide quantitation information were extracted from MaxQuant 1.5.2.8.[23] All the samples were searched against the Uniprot mouse database 2014-10 (*ftp://ftp.uniprot.org/pub/databases/uniprot*). Cleavage specificity was set for trypsin/P. Search parameters were two missed cleavage sites, cysteine carbamidomethylation as fixed modification and methionine oxidation as variable modification. Quantification data of labeled peptides were measure considering N-termini and lysine dimethylation on light (+28Da) or medium (+32Da) or on heavy (+36Da) modification per free primary amine.[21] The mass accuracy of the precursor ions was set by the recalibration algorithm of MaxQuant, fragment ion mass tolerance was set as default. The false discovery rate (FDR) was determined using statistical methods contained in MaxQuant software package v.1.5.2.8 and uses the multiple hypotheses testing (Cox et al.[23] and Elias et al.[24]). The maximum false discovery rate (FDR) was 1% for proteins and peptides, the minimum peptide length was 7 amino acids for valid identification. All other parameters are settings by default in MaxQuant. Quantitative ratios were calculated and normalized by Max Quant software package. R software (Version 3.0.0., www.r-project.org) was used to calculate log2 ratios between syn and allo-transplanted groups, log10 of signal intensities and p-values of protein abundance changes. p-values <0.05 were chosen as statistically significant. Normalized ratios were used for differential expression analysis (up ≥1.3 or down ≤0.44).

Real-Time Deformability Cytometry

For measurements, cells were re-suspended in PBS containing 0.63% methylcellulose at a concentration of 1-2 x 10^6 cells/ml and filtered through a 70 µm cell strainer. The cell suspension was drawn into a syringe and connected to a microfluidic chip consisting of two reservoirs separated by a channel constriction (15 x 15 μm^2 cross-section, 330 µm length). Using a syringe pump, cells were flushed through the channel at a constant flow rate of 0.048 µl/sec and imaged at the end of the constriction. The cells were deformed by hydrodynamic shear stresses and

pressure gradients into a characteristic bullet-like shape. Cell cross-sectional area ($A = \pi r^2$) and circularity ($c = 2\sqrt{\pi A}/l$), where l is the cell perimeter ($l = 2\pi r$), were determined in real-time using an algorithm implemented in C/LabVIEW. The results were displayed as scatter plots of deformation ($D = 1 - c$), which defines the deviation of the cell shape from a perfect circle ($c = 1$), and size[3]. To exclude pre-deformation or size misinterpretation we measured the cells in an area of the microfluidic chip where no shear stress was applied (reservoir). Deformation was close to zero indicated by round shaped, non-deformed cells and cell size was the same as in the micro-channel (Fig. 4f insert). Statistical comparison of deformation was carried out with 1-dimensional linear mixed model analysis. One fixed and one random effect was considered, in order to analyze the difference between subsets of cells and to consider the replicates' variance, respectively. *P* values were determined by a likelihood ratio test, comparing the full model with a model lacking the fixed effect term.

Supplemental Figures

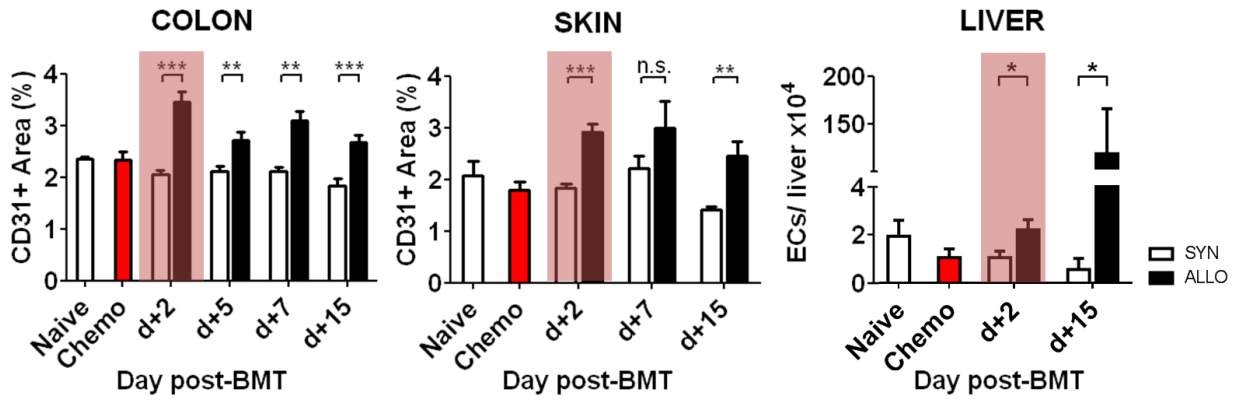

Figure S1. Time course of angiogenesis in GVHD target organs colon, skin and liver of syngeneic and allogeneic transplanted mice (LP/J→C57BL/6). Vascular density: Percentage of CD31 positive area in colon and skin and endothelial cell (EC) number in liver of syngeneic (SYN) and allogeneic (ALLO) transplanted mice at day+2, +5, +7 and +15 after BMT. The red box marks the earliest significant increase in positive CD31 areas or endothelial cell (EC) number in allogeneic transplanted mice. Untreated (Naive) and only chemotherapy-conditioned (Chemo) mice served as control and showed no increase in vascular density. Data pooled from two independent experiments (naive, chemo n=5 per group; SYN, ALLO n=10-12 per group). Error bars indicate mean ± s.e.m. **P* < 0.05, ***P* < 0.01, ****P* < 0.001, n.s. not significant by Student's *t* test (two-tailed).

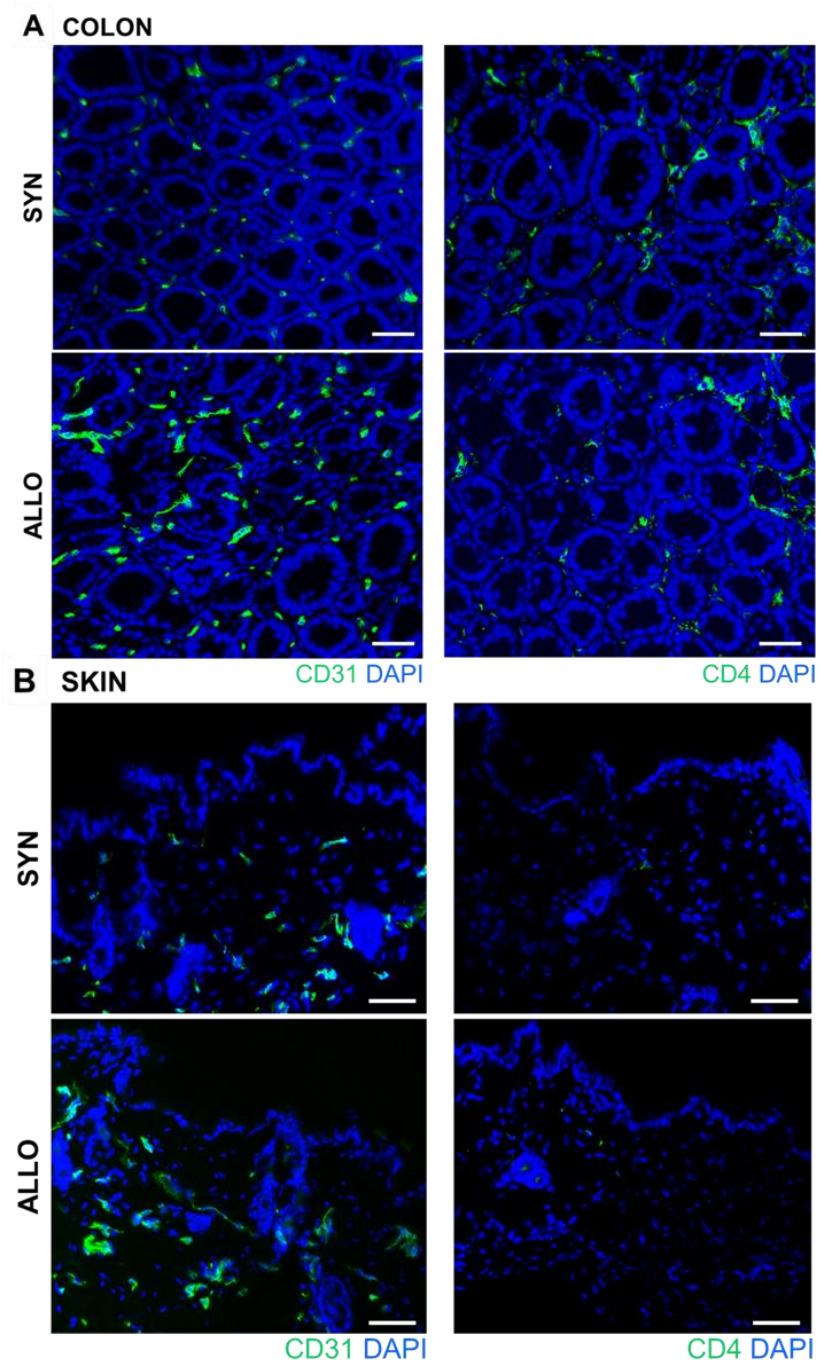

Figure S2. Increased vascular density and no CD4+ lymphocyte infiltration in colon and skin of allogeneic transplanted mice at day+2 after BMT. Representative pictures from colon (A) and skin (B) of SYN and ALLO mice at day+2 after BMT (LP/J→C57BL/6). Sections are stained against CD31 (green-A488) and CD4 (green-A488) and counterstained with 4´,6-Diamidino-2-phenylindole (DAPI). Scale bar, 30 µm.

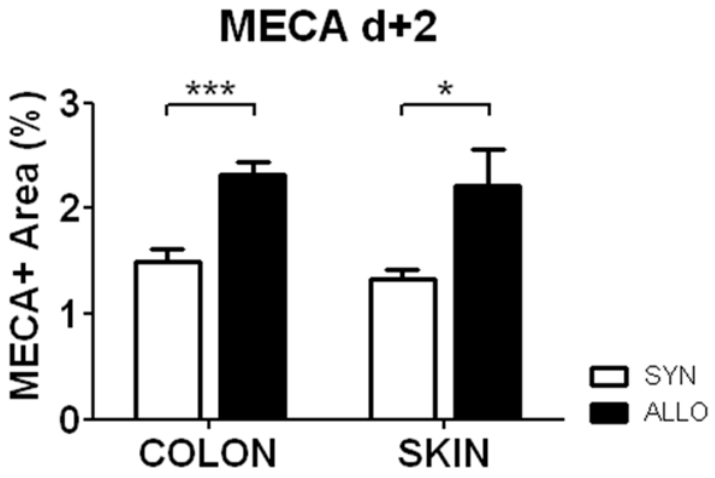

Figure S3. Staining with another endothelial cell marker MECA-32 confirms early angiogenesis in GVHD target organs. Increase in vascular density was determined by elevated positive areas of the stained endothelial cell marker MECA-32 in colon and skin of ALLO mice at day+2 after BMT (LP/J→C57BL/6). Representative data from one of two independent experiments (n=6 per group). Error bars indicate mean ± s.e.m. **P* < 0.05, ****P* < 0.001 by Student's *t* test (two-tailed).

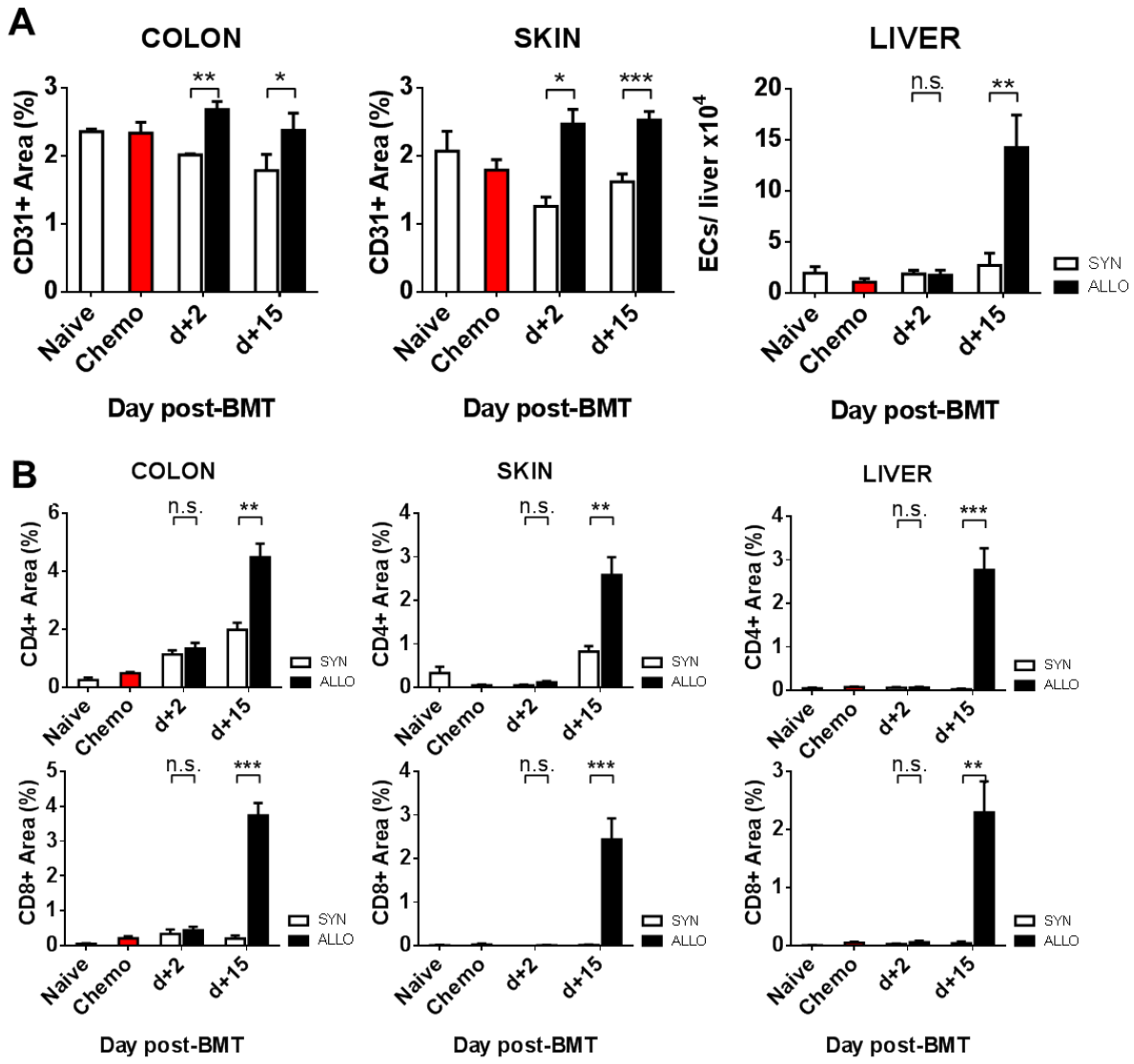

Figure S4. Angiogenesis precedes lymphocyte infiltration in another chemotherapy-based MHC-matched, miHA-mismatched murine GVHD model (129S2/SvPasCrl→C57BL/6). Time course of angiogenesis and lymphocyte infiltration in GVHD target organs colon, skin and liver of SYN and ALLO mice at day+2 and +15 after BMT. (A) Vascular density: Percentage of CD31 positive area in colon and skin and EC number in liver of SYN and ALLO mice. (B) Lymphocyte infiltration: Percentage of CD4 and CD8 positive area in colon, skin and liver of SYN and ALLO mice. Untreated (Naive) and only chemotherapy-conditioned (Chemo) mice served as control and showed no increase in vascular density or infiltration. Representative data from one of two independent experiments (n=5 per group). Error bars indicate mean ± s.e.m. *P < 0.05, **P < 0.01, ***P < 0.001, n.s. not significant by Student's *t* test (two-tailed).

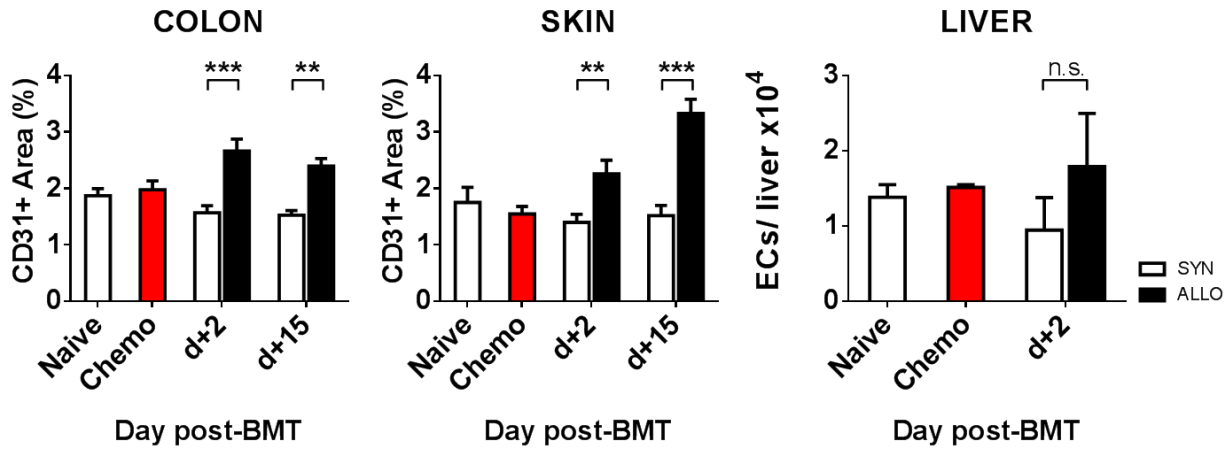

Figure S5. Early Angiogenesis in another chemotherapy-based MHC -mismatched murine GVHD model (C57BL/6→B6D2F1). Time course of angiogenesis in GVHD target organs colon, skin and liver of SYN and ALLO mice at day+2 and +15 after BMT. Vascular density: Percentage of CD31 positive area in colon and skin and EC number in liver of SYN and ALLO mice. CD4+ and CD8+ lymphocyte infiltration in GVHD target organs colon, skin and liver of ALLO mice was observed at day+15 but not at day+2 after BMT (data not shown). Untreated (Naive) and only chemotherapy-conditioned (Chemo) mice served as control and showed no increase in vascular density or infiltration. Representative data from one of two independent experiments (n=7 per group). Error bars indicate mean ± s.e.m. $^{**}P < 0.01$, $^{***}P < 0.001$, n.s. not significant by Student's *t* test (two-tailed).

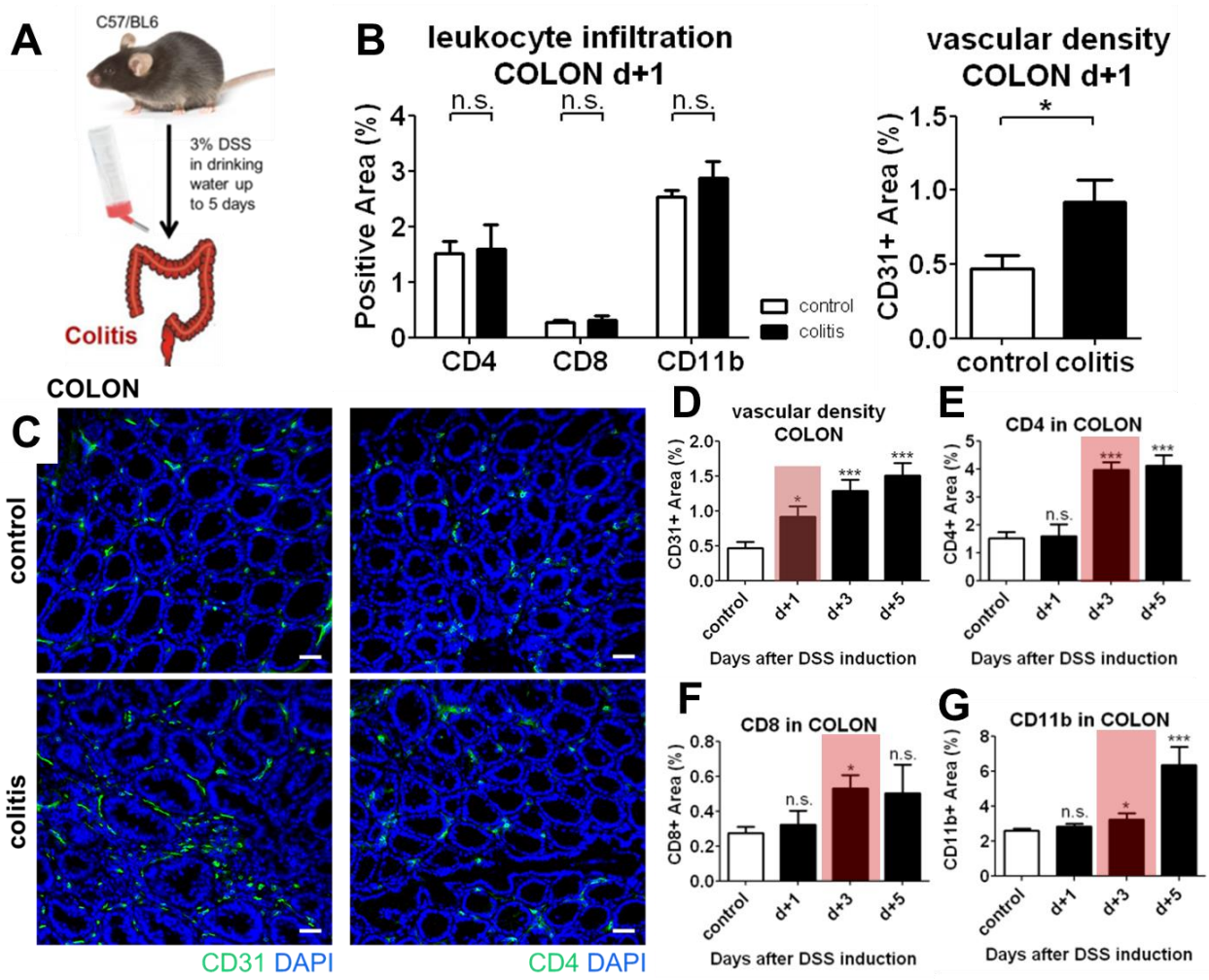

Figure S6. Angiogenesis precedes leukocyte infiltration during experimental colitis. (A) Schematic representation of induction of colitis with 3% dextran sulfate sodium (DSS). (B) Percentage of CD4, CD8, CD11b and CD31 positive area in colon of colitis bearing compared to control mice one day (d+1) after DSS induction. (C) Representative pictures from colon of colitis bearing and control mice at day+1 after DSS induction. CD31 (green-A488), CD4 (green-A488) and counterstained with DAPI. Scale bar, 30 µm. (D) Time course of angiogenesis in colon of colitis bearing mice compared to control mice. Control mice exhibited at all time points same percentage of CD31+ area. The red box marks the earliest significant increase in positive CD31 area in colitis bearing mice. (E, F, G) Time course of CD4+, CD8+, CD11b+ leukocyte infiltration. Red box marks the first significant increase in positive CD4, CD8 or CD11b area in colitis bearing mice. Representative data from one of two independent experiments (n=5-7 per group). Error bars indicate mean ± s.e.m. **P* < 0.05, ****P* < 0.001, n.s. not significant by Student's *t* test (two-tailed).

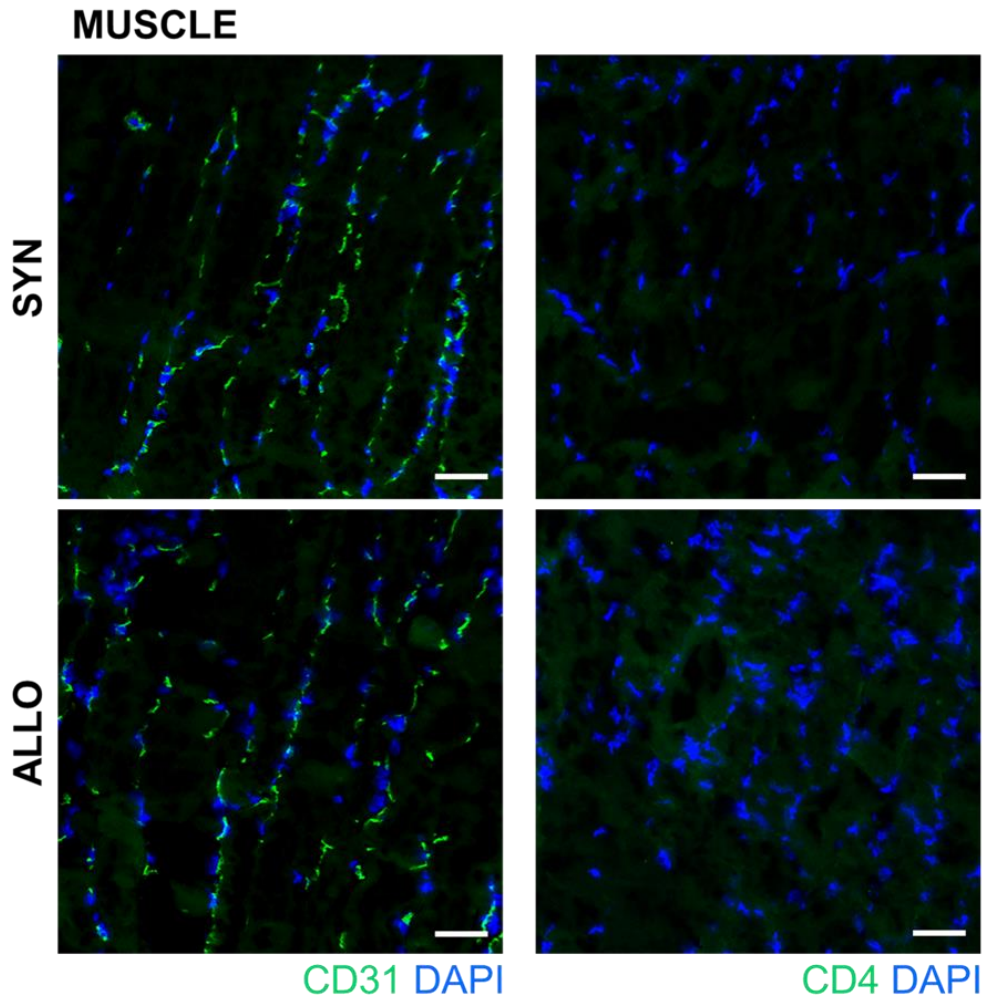

Figure S7. Non-target organs show no lymphocyte infiltration and no increase in vascular density. Representative pictures from skeletal muscle sections of SYN and ALLO mice at day+2 after BMT (LP/J→C57BL/6). Sections are stained against CD31 (green-A488) and CD4 (green-A488) and counterstained with DAPI. Scale bar, 30 µm.

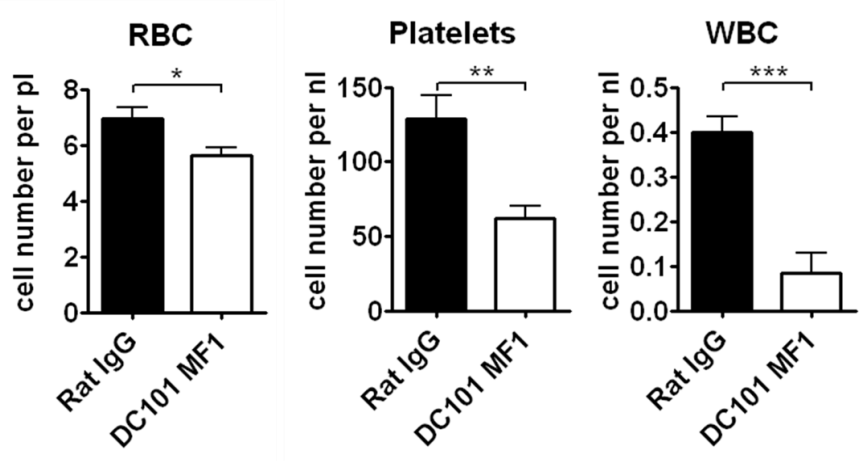

Figure S8. DC101+MFI treated mice showed significantly decreased hematological parameters suggesting defects in hematopoietic reconstitution. Hematological analysis of red blood cells (RBC), platelets and white blood cells (WBC) in peripheral blood of DC101+MF1 (VEGFR1+2 inhibitor) and rat IgG control treated mice at d+10 after BMT (C57BL/6→BALB/c). n=5 per group. Error bars indicate mean ± s.e.m. **P* < 0.05, ***P* < 0.01, ****P* < 0.001 by Student's *t* test (two-tailed).

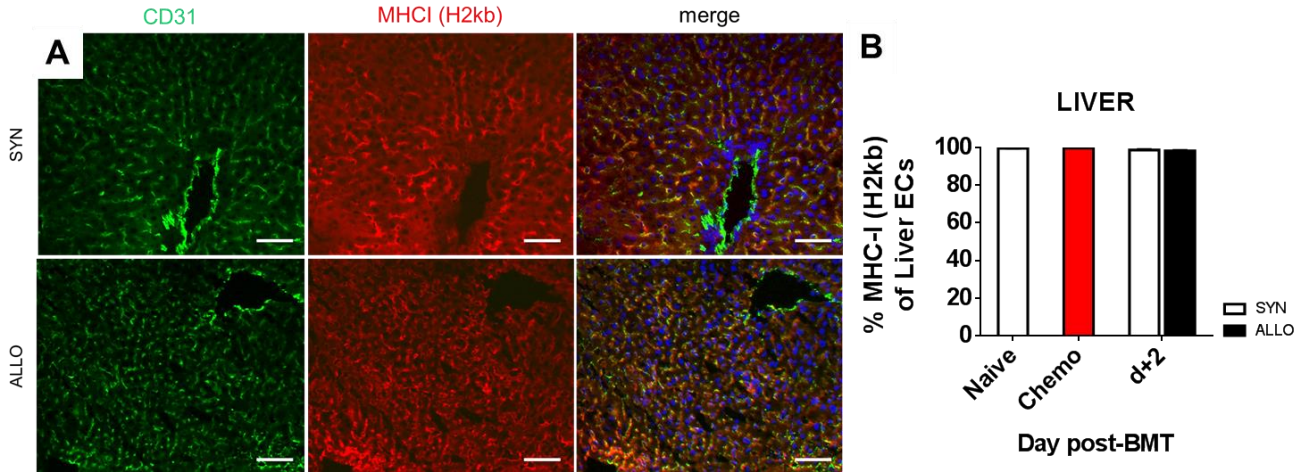

Figure S9. MHC-I expression in liver ECs (LP/J→C57BL/6). (A) Representative pictures from liver sections of SYN and ALLO mice at day+2 after BMT. Sections are stained against CD31 (green-A488), MHC-I (H2kb) (red-A555) and counterstained with DAPI. Scale bar, 30 µm. (B) FACS analysis of MHC-I (H2kb) on liver ECs of untreated (naive), chemotherapy-treated (Chemo) or SYN and ALLO mice at day+2 after BMT.

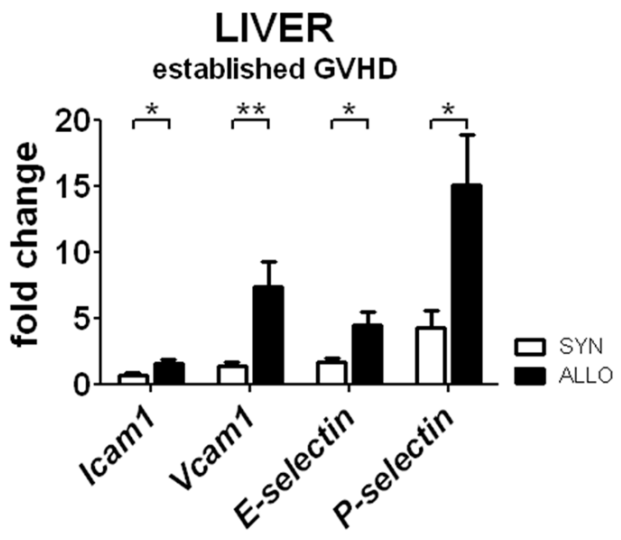

Figure S10. Increased expression of adhesion molecules in liver of allogeneic transplanted mice during established GVHD. Expression of adhesion molecules Intercellular Adhesion Molecule 1 (*Icam1*), vascular cell adhesion molecule 1 (*Vcam1*), *E-selectin* and *P-selectin* in ALLO versus SYN mice during established GVHD (GVHD scores >5) (LP/J→C57BL/6). Gene expression levels were normalized to *Gapdh* expression and are shown relative to gene levels of a reference untreated sample. n=10 per group. Error bars indicate mean ± s.e.m. **P* < 0.05, ***P* < 0.01 by Student's *t* test (two-tailed).

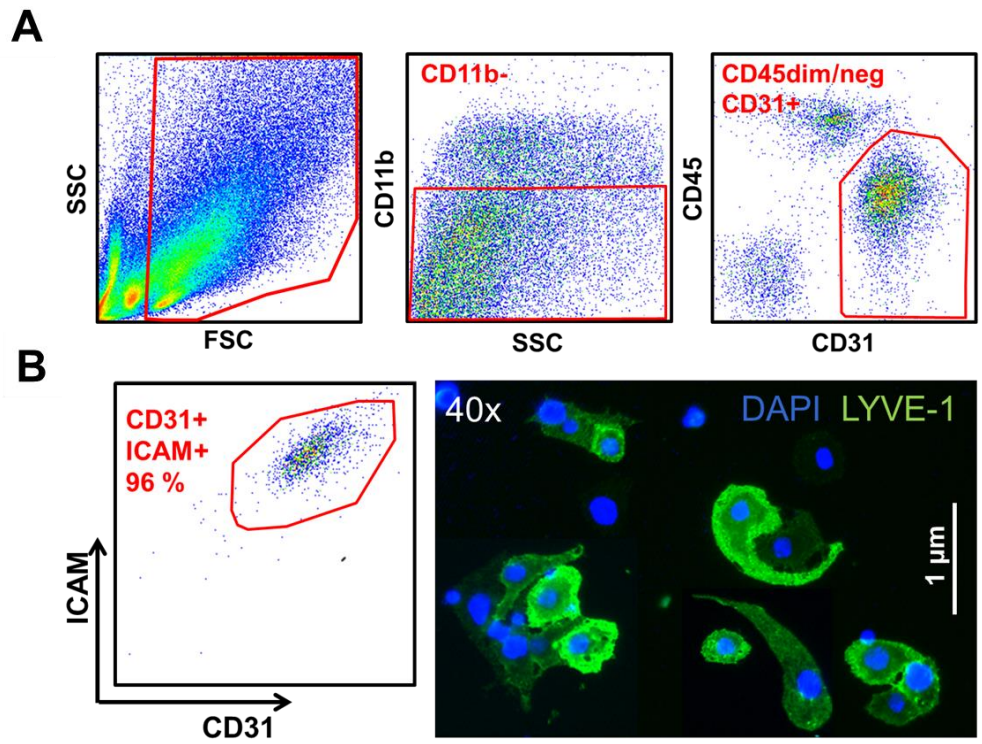

Figure S11. Gating Strategy and Purity check of MACS-isolated liver ECs and FACS-sorted colon ECs. (A) Endothelial cells were FACS-sorted as CD11b-CD45dim/-CD31+ cells. (B) Purity check by flow cytometry analysis of CD31 and ICAM1 revealed over 90 % purity. Some isolated ECs were plated on fibronectin-coated dishes. In 40x magnification isolated ECs exhibited positive LYVE-1 staining (green) and typical cell shape.

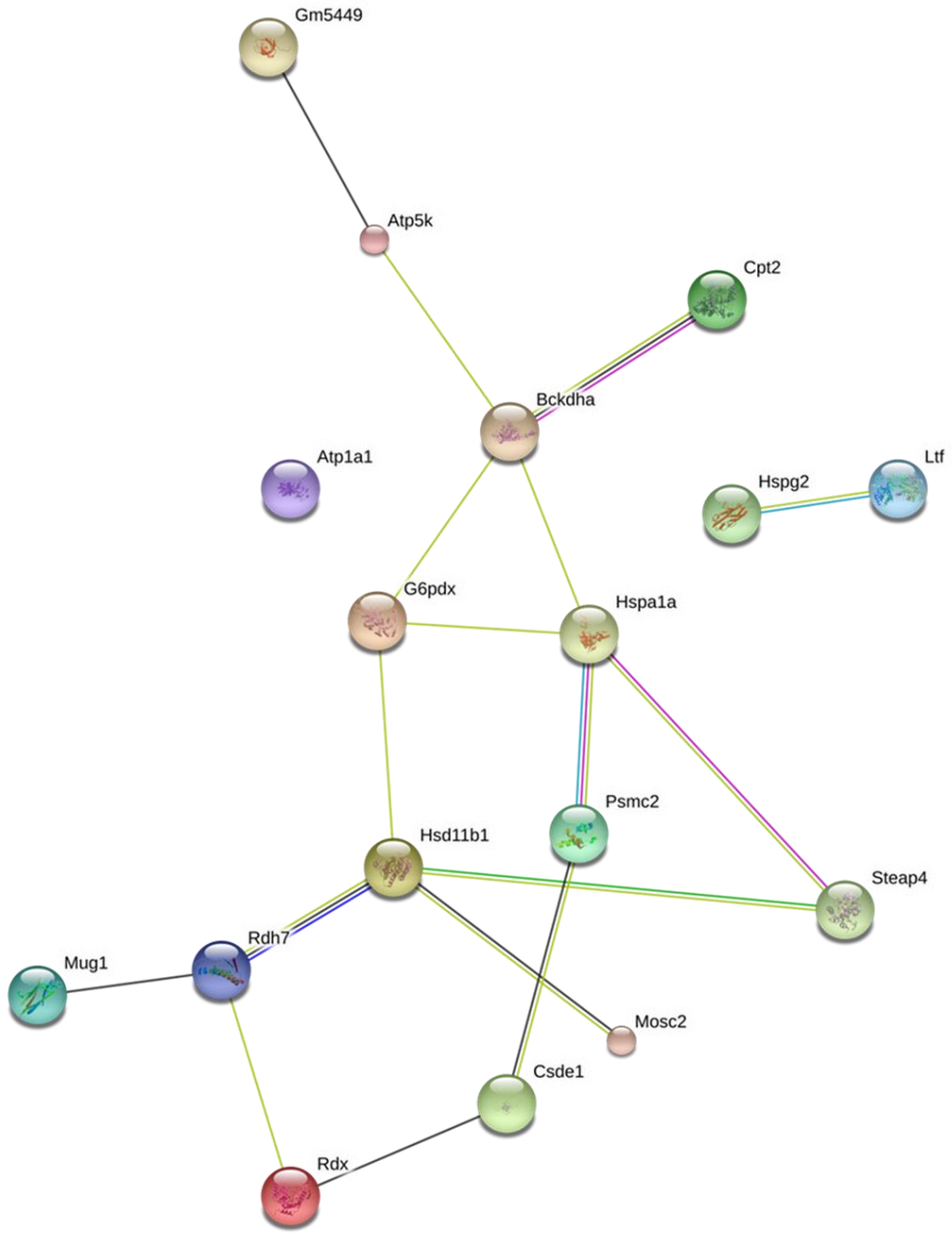

Figure S12. Network connections of the 18 up-regulated proteins in liver ECs of allogeneic transplanted mice at day+2 after BMT. Network connections were analyzed with http://string-db.org. Colored lines represent different interactions: known interactions from curated databases (cyan) and experimentally determined (violet); predicted interactions by gene neighborhood (green) and by gene co-occurrence (blue); by textmining (yellow) and co-expression (black).

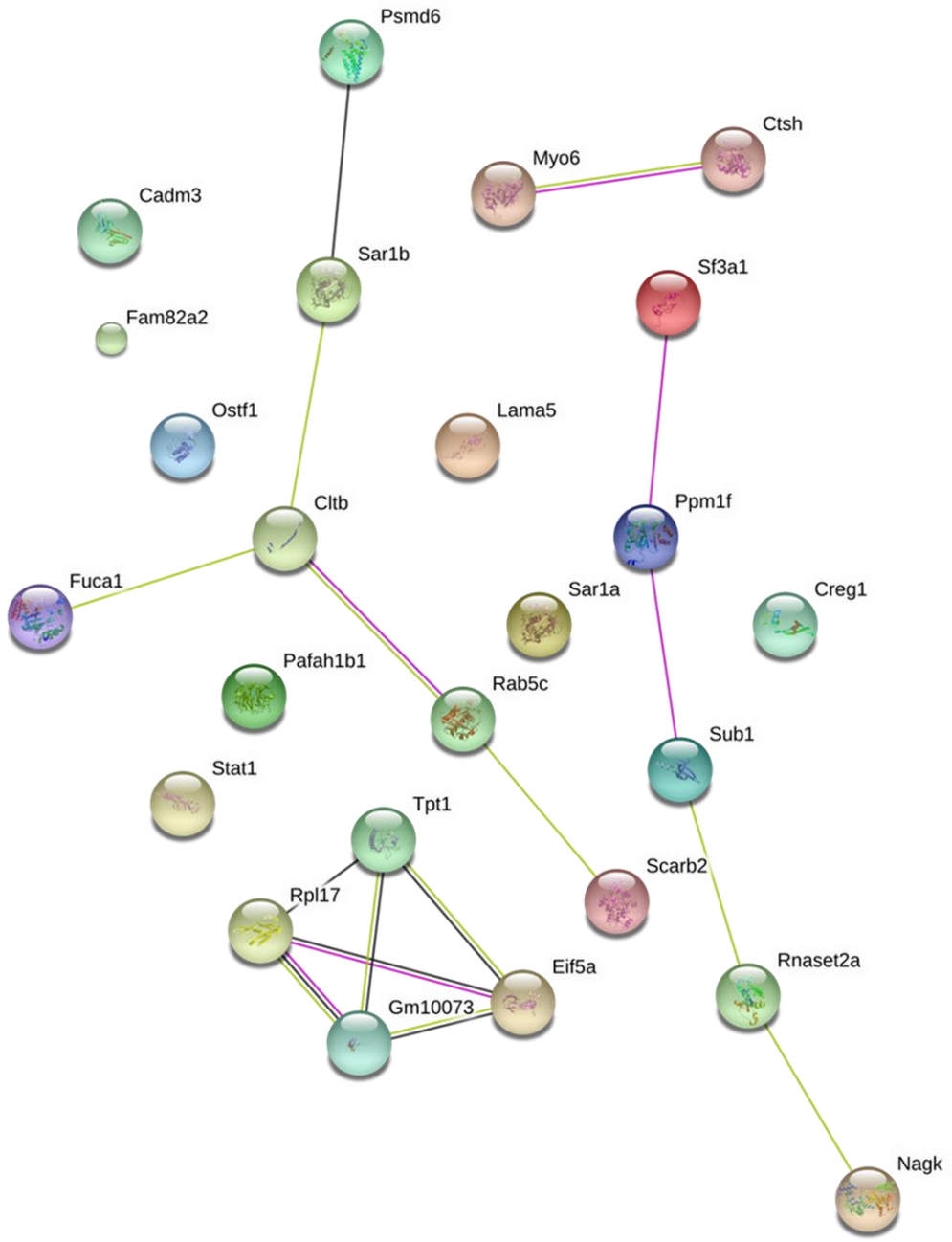

Figure S13. Network connections of the 25 down-regulated proteins in liver ECs of allogeneic transplanted mice at day+2 after BMT. Network connections were analyzed with http://string-db.org. Colored lines represent different interactions: known interactions from experimentally determined (violet); by textmining (yellow) and co-expression (black).